

Using ASTER satellite data to calculate riparian evapotranspiration in the Middle Rio Grande, New Mexico

A. S. BAWAZIR^{*†}, Z. SAMANI[†], M. BLEIWEISS[‡], R. SKAGGS[¶]
and T. SCHMUGGE[§]

[†]Civil and Geological Engineering, MSC 3CE, New Mexico State University,
PO Box 30001 Las Cruces, NM 88003-0083, USA

[‡]Entomology Plant Path and Weed Science, MSC 3BE, New Mexico State University,
PO Box 30001 Las Cruces, NM 88003-0057, USA

[¶]Agricultural Economics and Agricultural Business, MSC 3169, New Mexico State
University, PO Box 30001 Las Cruces, NM 88003-3169, USA

[§]College of Agriculture and Home Economics, MSC 3AG, New Mexico State University,
Las Cruces, NM 88003-0034, USA

(Received 27 August 2007; in final form 9 February 2008)

Riparian evapotranspiration (ET) in the Rio Grande Basin in New Mexico, USA is a major component of the hydrological system. Over a period of several years, ET has been measured in selected locations of dense saltcedar and cottonwood vegetation. Riparian vegetation varies in density, species and soil moisture availability, and to obtain accurate measurements, multiple sampling points are needed, making the process costly and impractical. An alternative solution involves using remotely sensed data to estimate ET over large areas. In this study, daily ET values were measured using eddy covariance flux towers installed in areas of saltcedar and cottonwood vegetation. At these sites, remotely sensed satellite data from the National Aeronautics and Space Administration (NASA) Terra Advanced Spaceborne Thermal Emission and Reflection Radiometer (ASTER) were used to calculate the albedo, normalized difference vegetation index (NDVI) and surface temperature. A surface energy balance model was used to calculate ET values from the ASTER data, which were available for 7 days in the year. Comparison between the daily ET values of saltcedar and cottonwood measured from the flux towers and calculated from remote sensing resulted in a mean square error (MSE) of 0.16 and 0.37 mm day^{-1} , respectively. The regional map of ET generated from the remote sensing data demonstrated considerable variation in ET, ranging from 0 to 9.8 mm day^{-1} , with a mean of 5.5 mm day^{-1} and standard deviation of 1.85 mm day^{-1} ($n = 427481$ pixels) excluding open water. This was due to variations in plant variety and density, soil type and moisture availability, and the depth to water table.

1. Introduction

Riparian evapotranspiration (ET) in the Rio Grande Basin has become a major hydrological as well as a political issue in New Mexico. The state of New Mexico and the US federal government have spent millions of dollars in recent years to remove and control exotic saltcedar (*Tamarix* spp.) vegetation in riparian regions without being able to

*Corresponding author. Email: abawazir@nmsu.edu

quantify the change in regional ET or the effect of its control on the hydrology of the basin. For decades, several studies have focused on measuring ET of individual riparian vegetation types in selected locations, mainly dense saltcedar (Blaney and Hanson 1965, van Hylckama 1974, Gay and Fritsch 1979, Sala *et al.* 1996, Devitt *et al.* 1998, Bawazir 2000, Cleverly *et al.* 2002) and native cottonwood (Gatewood *et al.* 1950, Blaney and Hanson 1965, Unland *et al.* 1998, Bawazir 2000). There are various methods for estimating ET. Some of these methods are well documented and have been described by Jensen *et al.* (1990) and Dingman (2002). The most common approach used in agriculture is to calculate the reference crop evapotranspiration (ET_o) and multiply it by a crop coefficient, K_c (Allen *et al.* 1998). In this procedure, ET_o is generally defined as the evapotranspiration from well-watered grass and the actual ET of the crop is calculated as:

$$ET = K_c \times ET_o \quad (1)$$

Various equations have been developed to estimate ET_o from weather data. These equations range from complex theoretical equations such as Penman-Monteith (Jensen *et al.* 1990, Allen *et al.* 1998) to simpler equations that use one or two climatic parameters (Priestly and Taylor 1972, Hargreaves and Samani 1982, 1985).

Crop coefficient values have been developed by various investigators based on direct field measurement of ET. This traditional method of estimating ET assumes that the vegetation is growing under optimum conditions and does not account for the impact of stress. The stress could be caused by water shortage, disease or other adverse environmental factors such as nutrient deficiencies. The traditional method of estimating vegetation ET from reference ET is not practical in the arid southwest riparian settings because of limited soil moisture and variability in vegetation density, mixture and age.

Currently available crop coefficients are limited to specific riparian vegetation and density with the assumption that it is growing under optimum soil moisture conditions. The recent advances in remote sensing technology have provided an opportunity to estimate vegetation ET from remotely sensed data using a surface energy balance scheme (Bastiaanssen *et al.* 1998a, b, Allen 2000). Knowledge of the surface energy balance can be used to estimate ET regardless of stress and does not require detailed soil and crop water information. In addition, estimating ET with satellite data is not limited to point measurements of ET and can be used to provide large-scale ET estimates. The work presented here demonstrates the application of remote sensing technology using Advanced Spaceborne Thermal Emission and Reflection Radiometer (ASTER) data combined with readily available ground weather data measurements to estimate riparian vegetation ET. The results are compared to ground level ET measured by eddy covariance flux towers.

2. Field measurements to calculate ET

The study site was located in the Middle Rio Grande floodplain at Bosque del Apache National Wildlife Refuge (Bosque), about 21 km south of Socorro in central New Mexico, USA. A 12-m eddy covariance flux tower was installed in the saltcedar (latitude $33^{\circ} 47' 14.24''$ N; longitude $-106^{\circ} 52' 35.79''$ W) and a 15-m tower was installed in the cottonwood site (latitude $33^{\circ} 47' 25.30''$ N; longitude $-106^{\circ} 52' 44.85''$ W). The saltcedar at the study site was at least 80 ha, with an average width of about 350 m. Saltcedar trees at the study site are very dense, with heights ranging between 6 and 7 m. Adjacent to the saltcedar site was the cottonwood. The cottonwood was planted from tree poles in 1991 (Taylor and McDaniel 1998) and covered

an area of about 61 ha with a width of approximately 200 m. The height of the cottonwood trees ranged between 9 and 10 m. In addition to the cottonwood trees, the area was composed of some understorey vegetation such as lambsquarters (*Chenopodium album*), jimsonweed (*Datura stramonium*), western ragweed (*Ambrosia psilostachya*), sporadic saltcedar-growth in sunny areas and other low-growing herbaceous plants.

The eddy covariance technique, using one-propeller eddy covariance (OPEC) systems, was used on the towers to measure the sensible heat (H) component of the surface energy. The OPEC sensors were placed about 7 m above the saltcedar canopy and about 6 m above the cottonwood canopy. The eddy covariance technique estimates sensible heat flux at the surface from the covariance between the fluctuations of vertical wind speed with temperature. Assuming that the mean vertical wind speed is zero, turbulent fluxes of sensible heat can be expressed as:

$$H = \rho_a c_p \text{COV} (wT) \quad (2)$$

where H is the sensible heat flux to the air (W m^{-2}), ρ_a is the air density (g m^{-3}), c_p is the heat capacity of air at constant pressure ($\text{J g}^{-1} \text{ }^\circ\text{C}$), w is the vertical air velocity (m s^{-1}), T is temperature of the air ($^\circ\text{C}$) and COV is the covariance between w and T during the sampling period. Data were collected at 8 Hz and statistical summaries of 30-min means were processed online using battery-powered CR23X data loggers (Campbell Scientific Inc., Logan, Utah, USA).

The ground heat flux (G) was measured using soil heat flux plates (model HFT3, REBS Inc., Belleville, Washington, USA) under the plant canopies. The ground heat flux plates were placed about at 1 cm in the ground at a location that best represented both open and shaded canopies. Changes in heat storage in the upper 1 cm layer of soil were assumed to be negligible and the mean soil heat flux measured was accepted. Net radiation (R_n) was measured using net radiometers (Model Q7.1, REBS Inc.) mounted about 2.5 m above the canopy. The latent heat flux (L) was determined as a residual in the energy balance as follows:

$$L = R_n - G - H \quad (3)$$

where all components are in W m^{-2} . The 30-min data were later analysed and integrated over 24 h to calculate the daily observed ET.

The ET was determined by dividing the latent heat flux by the latent heat of vaporization of water ($2.45 \times 10^6 \text{ J kg}^{-1}$ or $\text{W kg}^{-1} \text{ s}$ at 20°C). The polarity of the fluxes is such that R_n is positive when the sense is towards the exchange surface and L , G and H are positive when the sense is away from the exchange surface.

3. Remote sensing model to estimate ET

The satellite images used in this study were from the ASTER onboard the National Aeronautics and Space Administration (NASA) Terra satellite (Yamaguchi *et al.* 1998), which has a 60-km swath and a 16-day repeat cycle. However, images are not always available on a 16-day cycle at all locations. Satellite images from ASTER were used to calculate the albedo, the normalized difference vegetation index (NDVI) and the surface temperature for the study site. The ASTER sensor makes multispectral observations in three wavelength regions: visible to near-infrared (VNIR), shortwave

infrared (SWIR) and thermal infrared (TIR). The ASTER data used in this study came from the Land Processes Distributed Active Archive Center (LPDAAC; <http://lpdaac.usgs.gov/main.asp>) and consisted of AST_07 surface reflectance products with 15 m (VNIR) and 30 m (SWIR) spatial resolution and AST_08 surface kinetic temperature products with 90 m resolution.

The data were time-referenced and annotated with ancillary information, including radiometric and geometric calibration coefficients, and geolocation information. In addition, the data were corrected for parameters such as atmospheric effects and variations in emissivity. The remote sensing software package ENVI® (Research Systems, Inc., Boulder, CO, USA) and its tools were used for the data processing described here. The NDVI was calculated using ASTER sensor bands 3 and 2 as:

$$\text{NDVI} = \frac{\rho_3 - \rho_2}{\rho_3 + \rho_2} \quad (4)$$

where ρ_2 is the reflectance in band 2 and ρ_3 the reflectance in band 3.

Albedo (α) was calculated using the methodology described by Liang (2001):

$$\alpha = 0.484\rho_1 + 0.335\rho_3 - 0.324\rho_5 + 0.551\rho_6 + 0.305\rho_8 - 0.367\rho_9 - 0.0015 \quad (5)$$

where $\rho_1, \rho_3, \rho_5, \rho_6, \rho_8$ and ρ_9 are reflectance in bands 1, 3, 5, 6, 8 and 9, respectively.

Incident net radiation (R_{ni}) values (in W m^{-2}) for the time of satellite overpass, which was about 1100 h mountain standard time, were calculated after Campbell (1977) as:

$$R_{ni} = [(1 - \alpha)R_{si\downarrow}] + [\varepsilon_a\sigma(T_a + 273) - \varepsilon_s\sigma(T_s + 273)] \quad (6)$$

where $R_{si\downarrow}$ is the incident incoming shortwave radiation (W m^{-2}) measured at a weather station near the study site, σ is the Boltzmann constant ($5.67 \times 10^{-8} \text{ W m}^{-2} \text{ K}^{-4}$), T_a and T_s are the air and aerodynamic surface temperatures (in $^{\circ}\text{C}$), respectively, ε_s is the surface emissivity (set to 0.98) and ε_a is the atmospheric emissivity (calculated as $0.72 + 0.005 T_a$).

The incident soil heat flux (G_i) at 1100 h was calculated using an equation recommended by Samani *et al.* (2005) as:

$$\frac{G_i}{R_{ni}} = 0.26 \exp [-1.97(\text{NDVI})] \quad (7)$$

where G_i represents the soil heat flux at 1100 h (when the ground is heating up). Choudhury (1991) recommended an equation similar to equation (7) where the ratio of G_i/R_{ni} was calculated from values of the leaf area index (LAI).

The incident sensible heat flux (H_i) was calculated iteratively after Tasumi (2003) by combining the aerodynamic equation with the Monin–Obukhov length parameter as an indicator of atmospheric stability:

$$H_i = \rho_a C_p \frac{T_s - T_a}{r_{ah}} = \rho_a C_p \frac{dT}{r_{ah}} \quad (8)$$

where ρ_a is the air density (kg m^{-3}), C_p is the specific heat of air ($1004 \text{ J kg}^{-1} \text{ K}^{-1}$), T_s is the aerodynamic surface temperature (K), T_a is the air temperature (K), dT is the differential temperature between T_s and T_a , and r_{ah} is the aerodynamic surface resistance to heat transport (s m^{-1}). Equation (8) was combined with the

Monin–Obukov stability function to solve for dT and r_{ah} using two reference points. A relationship was developed between dT and T_s as:

$$dT = aT_s + b \quad (9)$$

where a and b are calibration coefficients for each day. To calculate a and b , two areas of known ET were selected. One area was the footprint of an independent flux tower (latitude $33^{\circ} 46' 52.11''$ N; longitude $-106^{\circ} 52' 38.23''$ W) in a dense monotypic saltcedar and the other was a dry ploughed field with no vegetation where ET was assumed to be zero. Equations (8) and (9) and the Monin–Obukhov function were solved simultaneously to obtain the incident sensible heat flux (H_i).

The evaporative fraction (E_f) for each pixel is defined as the ratio of the latent heat flux to the available energy and is calculated using the values for H_i , G_i and R_{ni} :

$$E_f = \frac{R_{ni} - G_i - H_i}{R_{ni} - G_i} \quad (10)$$

Once E_f is calculated and assuming that it is constant over the 24-h period, the daily ET can be calculated by multiplying E_f by the daily available energy after Bastiaanssen *et al.* (2005) as:

$$\text{ET} = E_f(R_n - G) \quad (11)$$

Assuming a negligible daily G value (Allen *et al.* 1998, Bastiaanssen *et al.* 2005), daily ET can be calculated simply by multiplying E_f by the daily net radiation (R_n). R_n (in $\text{MJ m}^{-2} \text{ day}^{-1}$) was calculated using a methodology recommended by Samani *et al.* (2005) as:

$$R_n = R_{ni} \left(\frac{R_s}{R_{si}} \right) \quad (12)$$

where R_{ni} is the incident clear sky net radiation (W m^{-2}) calculated from equation (6), R_s is the daily shortwave solar radiation ($\text{MJ m}^{-2} \text{ day}^{-1}$) and R_{si} is the incident shortwave solar radiation (W m^{-2}). Values of R_s and R_{si} can be obtained from a nearby weather station.

4. Results and analysis

The energy budgets at the saltcedar and cottonwood sites are shown in figures 1 and 2, respectively. The sign convention was that positive values of RA (extraterrestrial radiation), R_n , R_{so} , and R_s (extraterrestrial, net radiation, clear sky solar radiation and global solar radiation) indicate energy moving towards the surface while positive values of L , G , and H (Latent, soil and sensible heat fluxes) indicate energy moving away from the surface. The energy budget indicates leaf emergence in early spring and senescence in the late part of the growing season. The sensible heat (H) declines as the leaves emerge, reaching a minimum value during full canopy cover. Conversely, the latent heat (L), which represents the ET, increases gradually with leaf emergence, peaks in late June, and then declines as the season progresses. Latent heat values in cottonwood (figure 2) declined rapidly after the peak due to a sudden fall in ground-water levels at the site resulting in stressed conditions.

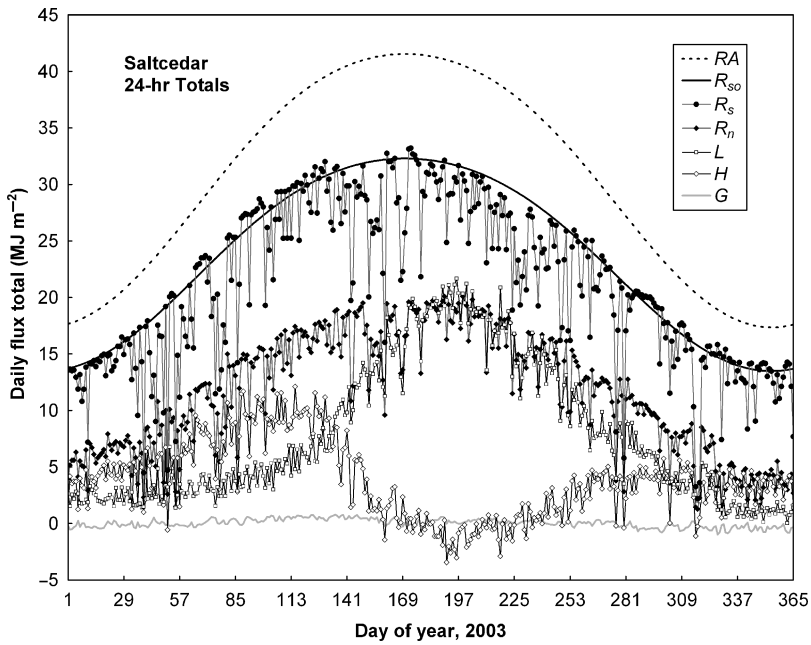


Figure 1. Daily flux measured at Bosque del Apache National Wildlife Refuge saltcedar site [RA: extraterrestrial radiation, R_{so} : clear sky solar radiation (Allen et al., 1998), R_s : global solar radiation, R_n : net radiation, H: sensible heat, L: latent heat, G: soil heat].

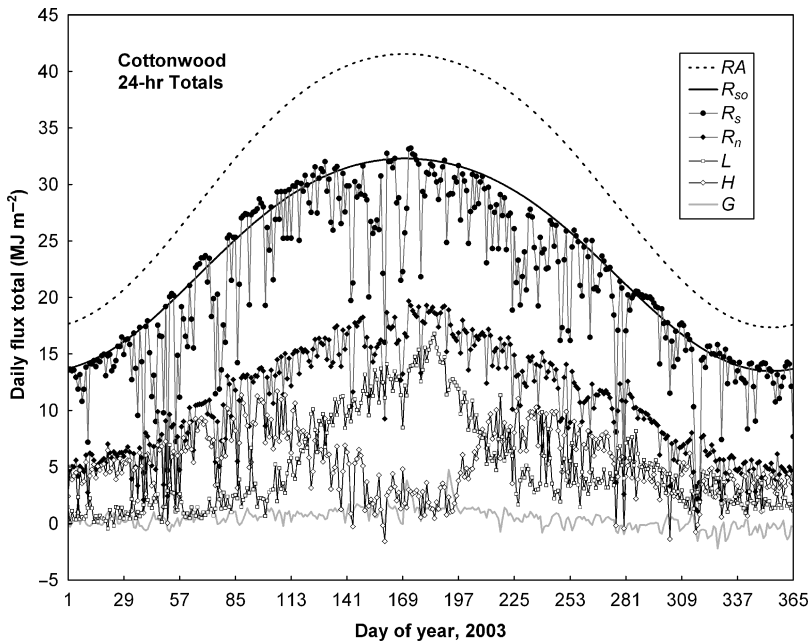


Figure 2. Daily flux measured at Bosque del Apache National Wildlife Refuge cottonwood site [RA: extraterrestrial radiation, R_{so} : clear sky solar radiation (Allen et al., 1998), R_s : global solar radiation, R_n : net radiation, H: sensible heat, L: latent heat, G: soil heat].

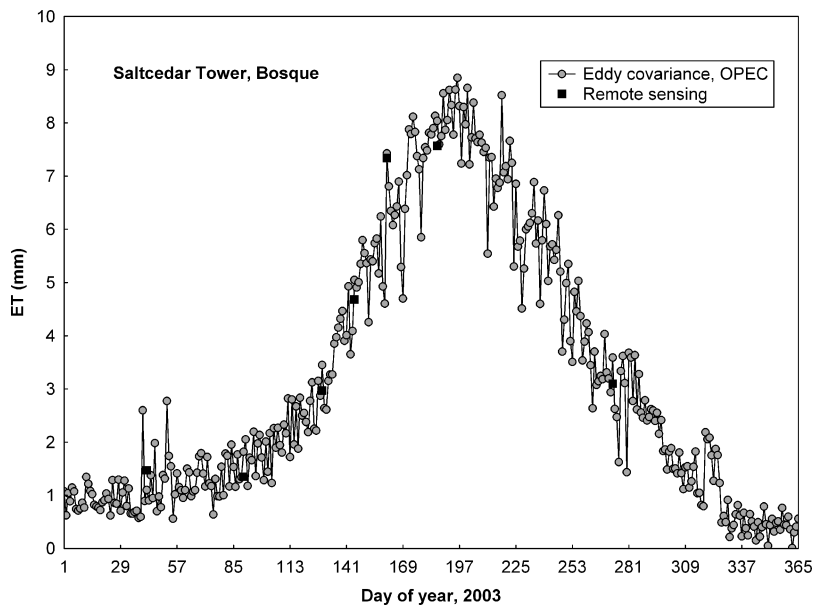


Figure 3. Comparison of saltcedar ET values predicted from remote sensing model with those measured by eddy covariance system at Bosque del Apache National Wildlife Refuge for the year 2003.

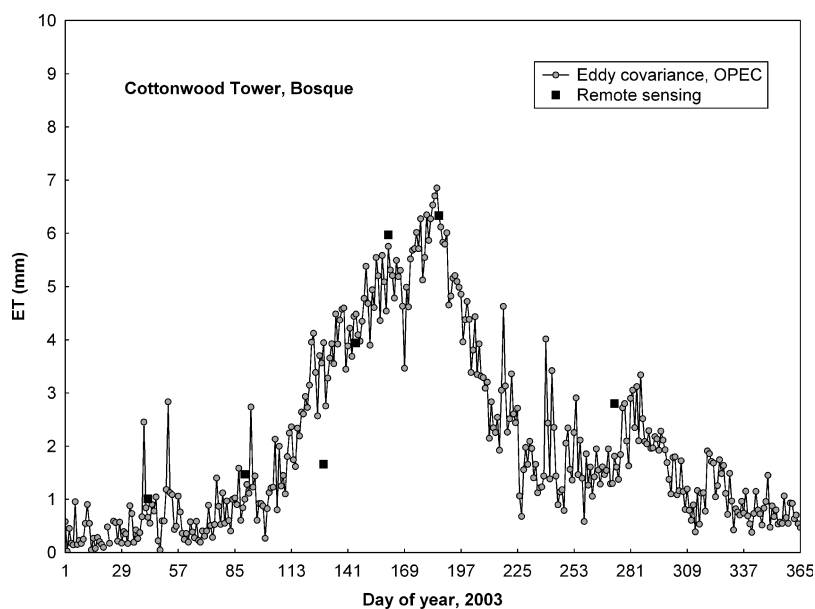


Figure 4. Comparison of cottonwood ET values predicted from remote sensing model with those measured by eddy covariance system at Bosque del Apache National Wildlife Refuge for the year 2003.

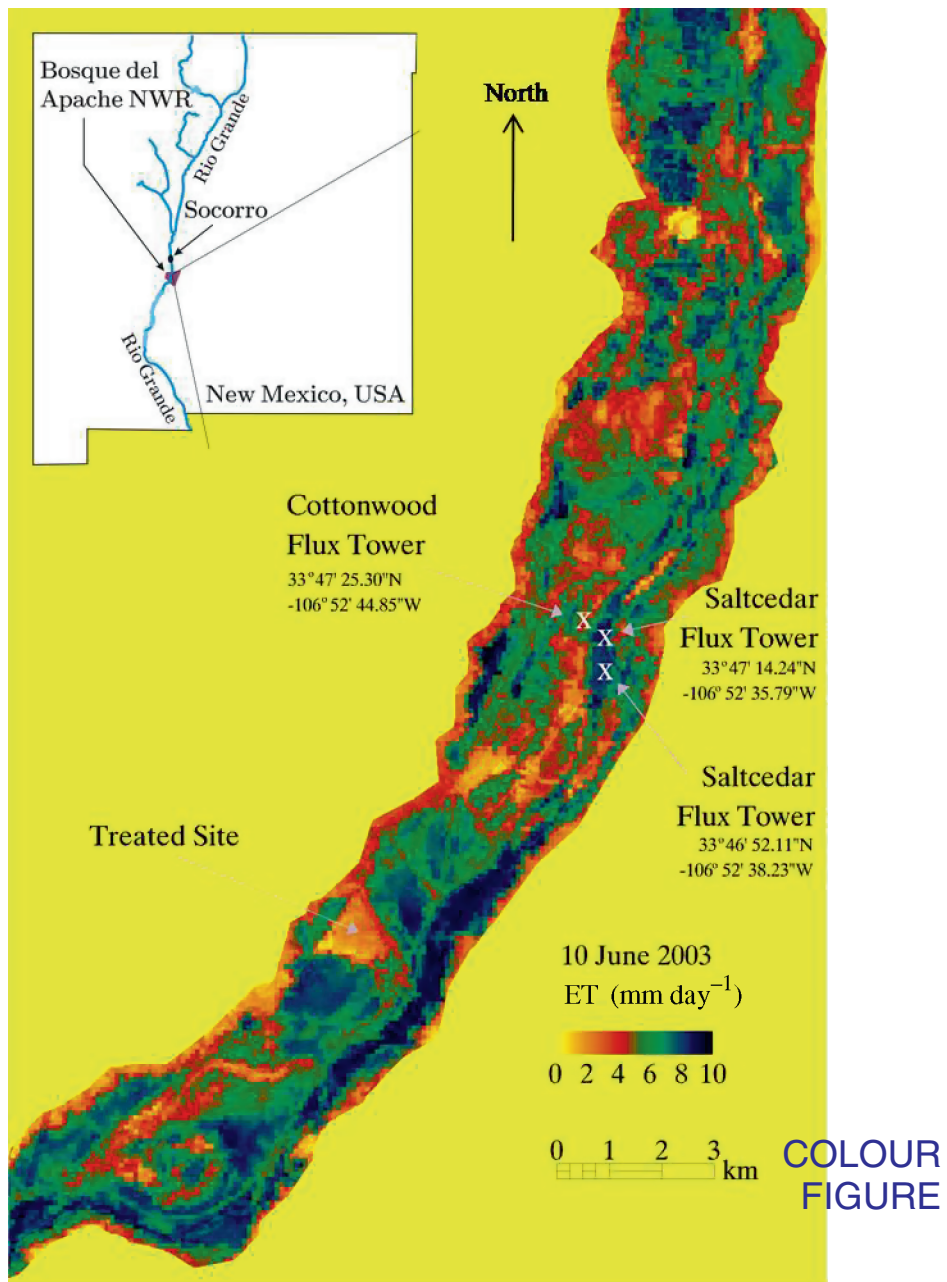


Figure 5. Regional map of ET for 10 June 2003 generated from remote sensing at Bosque del Apache National Wildlife Refuge (NWR), New Mexico, USA.

Measured values of riparian saltcedar and cottonwood ET using the eddy covariance method were compared to values predicted from the remote sensing model for the 7 days of the year when ASTER data were available. The comparisons are shown in figures 3 and 4. The remote sensing model can also be used to generate daily regional ET maps using satellite images for surface temperature, NDVI and albedo (see figure 5).

Table 1. Daily ET values measured with the flux tower, ET calculated from remote sensing, and ASCE standardized reference ET (ET_{sz}) calculated from local weather station data after Allen *et al.* (2005).

Date	Day of year	Saltcedar		Cottonwood		
		Flux tower (mm day ⁻¹)	Remote sensing (mm day ⁻¹)	Flux tower (mm day ⁻¹)	Remote sensing (mm day ⁻¹)	ET_{sz} (mm day ⁻¹)
11 February 2003	42	1.06	1.38	0.66	1.01	2.40
31 March 2003	90	1.29	1.53	1.01	1.47	5.73
9 May 2003	129	2.71	2.41	3.94	1.66	9.07
25 May 2003	145	4.48	4.42	4.48	3.94	8.49
10 June 2003	161	6.87	6.44	5.76	5.97	8.11
5 July 2003	186	7.56	7.12	6.35	6.33	7.85
30 September 2003	273	3.99	3.20	1.81	2.80	5.13
Average		3.99	3.79	3.43	3.31	6.68
MSE		0.16		0.37		

The mean squared error (MSE) was used as an indicator to compare the accuracy of prediction as:

$$MSE = \frac{\left[\sum_{i=1}^n ((ET_{est}) - (ET_m))^2 \right]^{\frac{1}{2}}}{n} \quad (13)$$

where ET_{est} is the estimated daily ET value from remote sensing, ET_m is the measured daily ET value from the flux tower, and n is the number of days ($n = 7$). The results of the flux measurements and remote sensing estimates for the 7 days are presented in table 1. MSE values were 0.16 and 0.37 mm day⁻¹ for saltcedar and cottonwood, respectively. Values of the American Society of Civil Engineers (ASCE) standardized reference evapotranspiration (ET_{sz}) or potential ET based on short vegetation (Allen *et al.* 2005) were calculated using weather station data located near the study site and are also presented in table 1. Annual precipitation for 2003 measured at the weather station was only 126 mm; normal annual precipitation for this location is about 200 mm per year.

The regional map of ET for 10 June 2003 generated from the remote sensing data is shown in figure 5, revealing variability of ET for the riparian region. ET estimates ranged from 0 to 9.8 mm day⁻¹, with a mean of 5.5 mm day⁻¹ and a standard deviation of 1.85 mm day⁻¹ ($n = 427\,481$ pixels) excluding open water. This was due to variations in plant variety and density, soil type and moisture availability, and the depth to water table. The depth to water table fluctuated during the year from 1 m during the winter to about 5 m during the summer months.

5. Conclusions

The work presented here demonstrates the application of remote sensing technology to estimate riparian vegetation ET. The results from remote sensing ET were compared to

ground-level ET measured by eddy covariance flux towers at Bosque National Wildlife Refuge in the Middle Rio Grande, New Mexico, USA. Eddy covariance flux towers were used to measure daily ET values in saltcedar and cottonwood. A remote sensing technique was used to calculate daily ET values based on surface energy balance for the same sites using data from the NASA/ASTER sensor. The results of the comparison showed MSE values of 0.16 mm day^{-1} for saltcedar and 0.37 mm day^{-1} for cottonwood. A regional map of ET during summer (10 June 2003) showed variability in ET ranging from 0 to 9.8 mm day^{-1} with a mean of 5.5 mm day^{-1} . Considering the diversity of vegetation and variations in soil moisture and groundwater levels, remote sensing provides a practical approach to calculating and monitoring riparian ET.

Acknowledgements

We acknowledge the support provided by the United States Bureau of Reclamation, United States Department of Fish and Wildlife Service, Bosque del Apache National Wildlife Refuge, United States Department of Agriculture Rio Grande Basin Initiative Project, New Mexico Office of the State Engineer/Interstate Stream Commission, and New Mexico Water Resources Research Institute. We also thank the New Mexico State University civil engineering students who maintained the flux towers and collected the data, and Vien D. Tran for generating the ET maps.

References

- ALLEN, R.G., 2000, *Prediction of ET in Time and Space for the Tampa Bay Region*. Unpublished report, Waterstone Environmental Hydrology and Engineering, Inc., Boulder, CO.
- ALLEN, R.G., PEREIRA, L.S., RAES, D. and SMITH, M., 1998, *Crop Evapotranspiration: Guidelines for Computing Crop Water Requirements* (Rome, Italy: Food and Agriculture Organization). FAO irrigation and drainage paper No. 56.
- ALLEN, R.G., WALTER, I.A., ELLIOTT, R., HOWELL, T., ITENFISU, D., JENSEN, M.E. and SNYDER, R.L., 2005, *The ASCE Standardized Reference Evapotranspiration Equation* (Reston, VA: American Society of Civil Engineers).
- BASTIAANSSEN, W.G.M., 2005, SEBAL model with remotely sensed data to improve water-resources management under actual field conditions. *Journal of Irrigation and Drainage Engineering*, **131**, pp. 85–93.
- BASTIAANSSEN, W.G.M., MENENI, M., FEDDES, R.A. and HOLTSLAG, A.A.M., 1998a, The surface energy balance algorithm for land (SEBAL): 1. Formulation. *Journal of Hydrology*, **212–213**, pp. 198–212.
- BASTIAANSSEN, W.G.M., PELGRUM, H., WANG, Y., MA, Y., MORENO, J.F., ROERINK, G.J. and VAN DER WAL, T., 1998b, A remote sensing surface energy balance algorithm for land (SEBAL): 2. Validation. *Journal of Hydrology*, **212–213**, pp. 213–229.
- BAWAZIR, A.S., 2000, Saltcedar and cottonwood riparian evapotranspiration in the Middle Rio Grande. PhD dissertation, New Mexico State University, Las Cruces, NM.
- BLANEY, H.F. and HANSON, E.G., 1965, Consumptive use and water requirements in New Mexico. *Technical Report of the New Mexico Office of the State Engineer*, **32**, pp. 1–82.
- CAMPBELL, G.S., 1977, *An Introduction to Environmental Biophysics* (New York: Springer).
- CHOWDHURY, B.J., 1991, Multispectral satellite data in the context of land surface heat balance. *Review of Geophysics*, **29**, pp. 217–236.
- CLEVERLY, J.R., DAHM, C.N., THIBAULT, J.R., GILROY, D.J. and ALLRED COONROD, J.E., 2002, Seasonal estimates of actual evapo-transpiration from *Tamarix ramosissima* stands using three-dimensional eddy covariance. *Journal of Arid Environments*, **52**, pp. 181–197.

- DEVITT, D.A., SALA, A., SMITH, S.D., CLEVERLY, J., SHAULIS, L.K. and HAMMETT, R., 1998, Bowen ratio estimates of evapotranspiration for *Tamarix ramosissima* stands on the Virgin River in southern Nevada. *Water Resources Research*, **34**, pp. 2407–2414.
- DINGMAN, S.L., 2002, *Physical Hydrology*, 2nd edn (Upper Saddle River, NJ: Prentice Hall).
- GATEWOOD, J.S., ROBINSON, T.W., COLBY, B.R., HEM, J.D. and HALFPENNY, L.C., 1950, Use of water by bottom-land vegetation in lower Safford Valley, Arizona. Geological Survey Water-Supply Paper 1103 (Washington, DC: United States Government Printing Office).
- GAY, L.W. and FRITSCHEN, L.J., 1979, An energy budget analysis of water use by saltcedar. *Water Resources Research*, **15**, pp. 1589–1592.
- HARGREAVES, G.H. and SAMANI, Z.A., 1982, Estimating potential evapotranspiration. *Journal of Irrigation and Drainage Engineering*, **108**, pp. 225–230.
- HARGREAVES, G.H. and SAMANI, Z.A., 1985, Reference crop evapotranspiration from temperature. *Journal of Applied Engineering in Agriculture*, **1**, pp. 96–99.
- JENSEN, M.D., BURMAN, R.D. and ALLEN, R.G., 1990, *Evapotranspiration and Irrigation Water Requirements*. ASCE Manuals and Reports on Engineering Practice No. 70 (New York: American Society of Civil Engineers).
- LIANG, S., 2001, Narrowband to broadband conversion of land surface albedo.I. Algorithms. *Remote Sensing of Environment*, **76**, pp. 213–238.
- PRIESTLY, C.H.B. and TAYLOR, R.J., 1972, On the assessment of surface heat flux and evaporation using large-scale parameters. *Monthly Weather Review*, **100**, pp. 81–92.
- SALA, A., SMITH, S.D. and DEVITT, D.A., 1996, Water use by *Tamarix ramosissima* and associated phreatophytes in a Mojave Desert floodplain. *Ecological Applications*, **6**, pp. 888–898.
- SAMANI, Z., NOLIN, S., BLEIWEISS, M. and SKAGGS, R., 2005, Discussion of ‘Predicting daily net radiation using minimum climatological data’. *Journal of Irrigation and Drainage Engineering*, **131**, pp. 338–389.
- TASUMI, M., 2003, Progress in operational estimation of regional evapotranspiration using satellite imagery. PhD dissertation, University of Idaho, Moscow, ID.
- TAYLOR, J.P. and McDANIEL, K.C., 1998, Restoration of saltcedar (*Tamarix* sp.)-infested floodplains on the Bosque del Apache National Wildlife Refuge. *Weed Technology*, **12**, pp. 345–352.
- UNLAND, H.E., ARAIN, A.M., HARLOW, C., HOUSER, P.R., GARATUZA-PAYAN, J., SCOTT, P., SEN, O.L. and SHUTTLEWORTH, W.J., 1998, Evaporation from a riparian system in a semi-arid environment. *Hydrological Processes*, **12**, pp. 527–542.
- VAN HYCKAMA, T.E.A., 1974, Water use by saltcedar as measured by the water budget method. Geological Survey Professional Paper 491-E (Washington, DC: United States Government Printing Office).
- YAMAGUCHI, Y., KAHLE, A.B., TSU, H., KAWAKAMI, T. and PNIEL, M., 1998, Overview of Advanced Spaceborne Thermal Emission and Reflection Radiometer (ASTER). *IEEE Transactions on Geoscience and Remote Sensing*, **36**, pp. 1062–1071.

